

Supplementary Information for

## **Membrane-curvature-mediated co-endocytosis of bystander and functional nanoparticles**

Kejie He,<sup>‡a</sup> Yushuang Wei,<sup>‡b</sup> Zhihong Zhang,<sup>a</sup> Haibo Chen,<sup>a</sup> Bing Yuan,<sup>\*a</sup> Hongbo Pang<sup>\*b</sup> and Kai Yang<sup>\*a</sup>

<sup>a</sup> Center for Soft Condensed Matter Physics and Interdisciplinary Research & School of Physical Science and Technology, Soochow University, Suzhou, 215006, P. R. China.

<sup>b</sup> Department of Pharmaceutics, University of Minnesota, Minneapolis, MN, USA.

<sup>‡</sup> These authors contributed equally to this work.

\* Correspondence to: yuanbing@suda.edu.cn; pang0051@umn.edu; yangkai@suda.edu.cn (K. Y.)

## Methods

**Potential of mean force calculation:** For a BNP-FNP-membrane system, the initial configurations between NPs adsorbing on a membrane with varying distances for umbrella sampling were generated by applying a spring force with the constant of 1000 J/mol/nm<sup>2</sup> to pull the BNP toward the FNP at a rate of 0.0001 nm/ps. Then the configuration windows spaced by 0.2 nm along the FNP-BNP connecting line were extracted from this trajectory, and thus the distance between FNP and BNP,  $L$ , could be chosen as the reaction coordinate. Umbrella sampling was initiated from each configuration. To obtain well-centered, overlapping histograms for umbrella sampling analysis, in each configuration window, the system was simulated for 400 ns by applying a spring force with the constant of 1000 J/mol/nm<sup>2</sup> between BNP and FNP to restrain the special NPs' configuration on the membrane. Then the first 100 ns of such trajectories was discarded and the PMF was obtained from the last 300 ns simulations using the Weighted Histogram Analysis Method as implemented in the program `g_wham` in the GROMACS package. Therefore, the calculated PMF profile reflects the free energy change of the system caused by the NP-membrane interactions at varying FNP-BNP distances.

**Energy analysis** (in the case with a tube-like endocytic vesicle form): We considered a NP-membrane system containing multiple FNPs (note that  $N_F$  is variable here) with a radius of  $r_F = 10 \text{ nm}$  and one BNP with the radius of  $r_B = 25 \text{ nm}$ . As shown in Fig S17, the `Config_t0` state refers to the state without the bystander effect, that is, all FNPs are wrapped by the membrane while the BNP is still left on the membrane surface without internalization. Here, the shape of the membrane-wrapped FNPs are assumed to be a tube with two hemispherical caps of radius  $R_0$  and a cylinder with length  $L_0$  (here we set  $L_0 = 2R_0$ ). Also, this tube has the same volume as that of the membrane-wrapped FNPs (i.e.,  $\frac{4}{3}\pi R_0^3 + \pi R_0^2 L_0 = N_F \frac{4}{3}\pi r_F^3$ ). The membrane wrapping degree of the BNP is assumed to be  $\eta_{B0}$ . Thus,

$$E_{t0} = \left( -\frac{4\pi R_0^2 + 2\pi R_0 L_0}{a_0} \mu_F + 10\kappa\pi \right) + \left( -\frac{4\pi r_B^2 \eta_{B0}}{a_0} \mu_B + 8\kappa\pi \eta_{B0} + \gamma 2\pi r_B \sqrt{4\eta_{B0}(1-\eta_{B0})} \right).$$

The first term on the right of (1) stems from the energy contribution of the FNP-membrane interactions and the second term is for the BNP. It is noted that there is also a ligand-receptor binding energy for BNP, although  $\mu_B \ll \mu_F$ . Here, we assume  $\mu_F = 20 k_B T$ ,  $\mu_B = 4 k_B T$ , and  $\eta_{B0} = 20\%$ . Note that the bending energy of a tube is  $E_{Bending} = 8\kappa\pi + \kappa\pi L_0/R_0 = 10\kappa\pi$ .

In contrast, the `Config_tB` state could be considered as an ideal bystander uptake state (Fig. S17). Also, the shape of these wrapped NPs (including both FNPs and BNP) is considered to be tube-like with caps radius  $R_1$  and length  $L_1$ . Thus,

$$E_b = \left( -\frac{4\pi R_1^2 + 2\pi R_1 L_1}{a_0} \mu_F + 10\kappa\pi \right).$$

In (2),  $R_1$  is the radius of the equivalent "tube", whose volume is  $\frac{4}{3}\pi R_1^3 + \pi R_1^2 L_1 = N_F \frac{4}{3}\pi r_F^3 + \frac{4}{3}\pi r_B^3$ .

Also, the partial bystander uptake state is considered. Here  $\eta_{un}$  is assumed to be the area ratio of the region at the top of the tube which is not wrapped by the membrane, which is about

$\eta_{un} = \left( \frac{4}{3}\pi R_c^3 + \pi R_c^2 L_c - N_F \frac{4}{3}\pi r_F^3 - \frac{4}{3}\pi r_B^3 \right) / \frac{4}{3}\pi R_c^3$  ( $R_c = 25 + 10 \times 2 = 45 \text{ nm}$  is the critical radius of a tube for fully wrapping BNP). Also, two possibilities are taken into consideration (Fig. S\*).

For state Config\_tP, the system energy is about:

$$E_{tp} = - \frac{(1 - \eta_{un})4\pi R_c^2 + 2\pi R_c L_c}{a_0} \mu_F + (10 - 8\eta_{un})\kappa\pi + \gamma 2\pi R_c \sqrt{4\eta_{un}(1 - \eta_{un})}$$

For state Config\_tP', the system energy is about:

$$E_{tp'} = - \frac{(1 - \eta_{un})4\pi R_c^2 + 2\pi R_c L_c}{a_0} \mu_F + 10\kappa\pi$$

For simplification, we only consider the situation with small  $\eta_{un}$  ( $\eta_{un} < 20\%$ ). Based on these considerations, the energy differences between the states associated with the bystander activity could be calculated as  $\Delta E_{tb} = E_{tb} - E_{t0}$ ,  $\Delta E_{tp} = E_{tp} - E_{t0}$ , and  $\Delta E_{tp'} = E_{tp'} - E_{t0}$ .

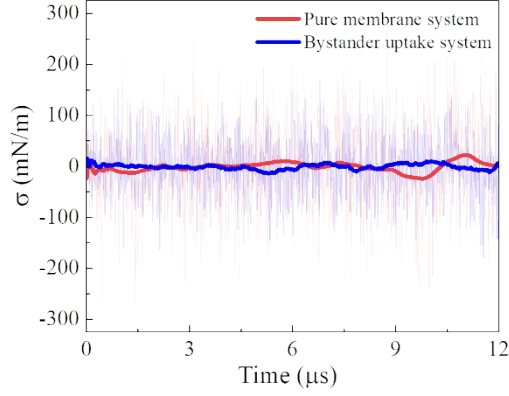


**Fig. S1** Analysis of membrane tension ( $\sigma$ ). Thick line is the central line of  $\sigma$  for highlight. Pure membrane system: DLPC lipid bilayer; Bystander uptake system: DLPC lipid bilayer + FNP/BNP ( $\epsilon_F = 3.5 \text{ kJ/mol}$ ,  $\epsilon_B = 1.5 \text{ kJ/mol}$ ,  $\rho_F = \rho_B = 1.6 \text{ nm}^{-2}$ ,  $D_F = D_B = 8 \text{ nm}$ ).

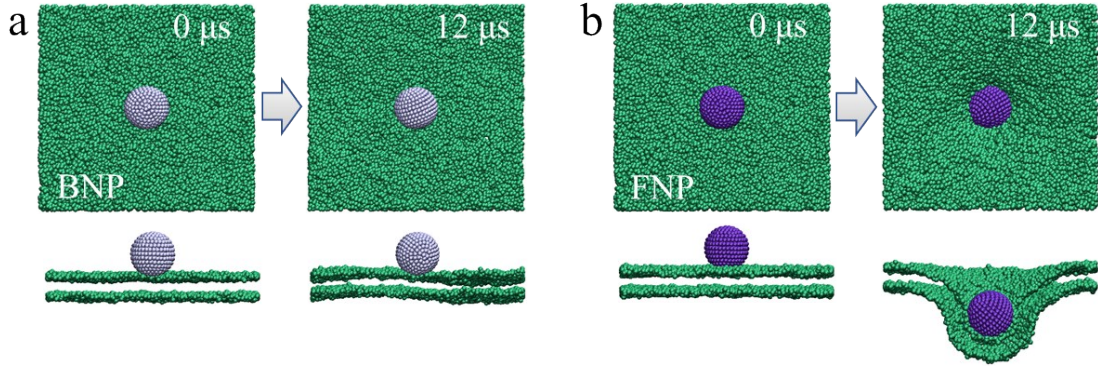


**Fig. S2** Representative snapshots during the NP-membrane interactions. (a) Adsorption of a BNP on the membrane without internalization. (b) Membrane wrapping of a FNP.  $\epsilon_F = 3.5 \text{ kJ/mol}$ ,  $\epsilon_B = 1.5 \text{ kJ/mol}$ ,  $\rho_F = \rho_B = 1.6 \text{ nm}^{-2}$ ,  $D_F = D_B = 8 \text{ nm}$ .

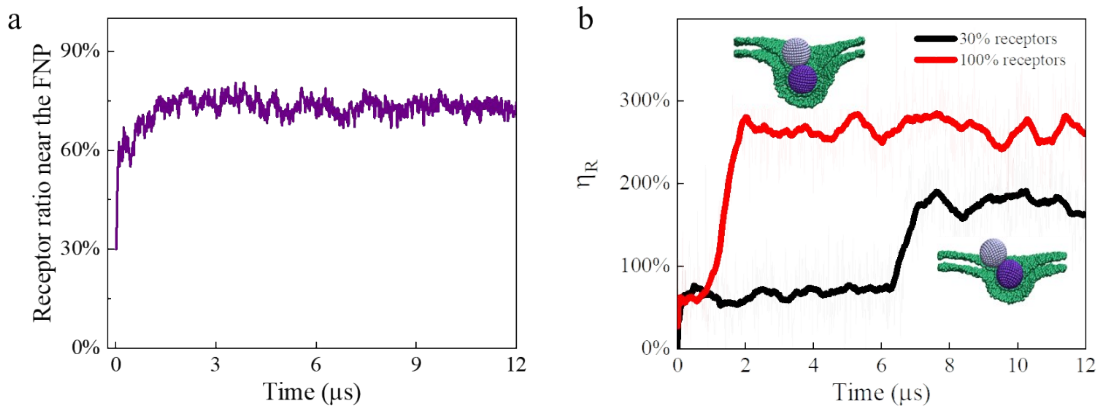


**Fig. S3** (a) Time evolution of the local number density of receptors around the membrane-bound FNP. The receptor ratio is initially set as 30% in the membrane. (b) Evolution of  $\eta_R$  with different receptor ratios (30% vs. 100%). Insets show the corresponding NP-membrane interaction situations at the end of the simulations in each condition.

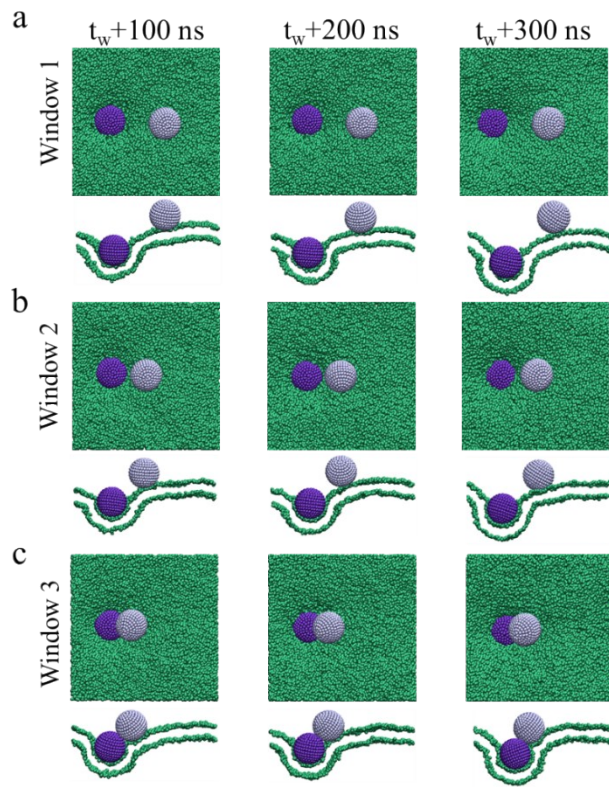


**Fig. S4** Snapshots showing the membrane morphologies at different simulation time points in a NP-membrane interaction configuration window (or at a certain FNP-BNP distance).  $\varepsilon_F = 3.5 \text{ kJ/mol}$ ,  $\varepsilon_B = 1.5 \text{ kJ/mol}$ ,  $\rho_F = \rho_B = 1.6 \text{ nm}^{-2}$ ,  $D_F = D_B = 8 \text{ nm}$ .  $t_w$  refers to the beginning time point of the window.

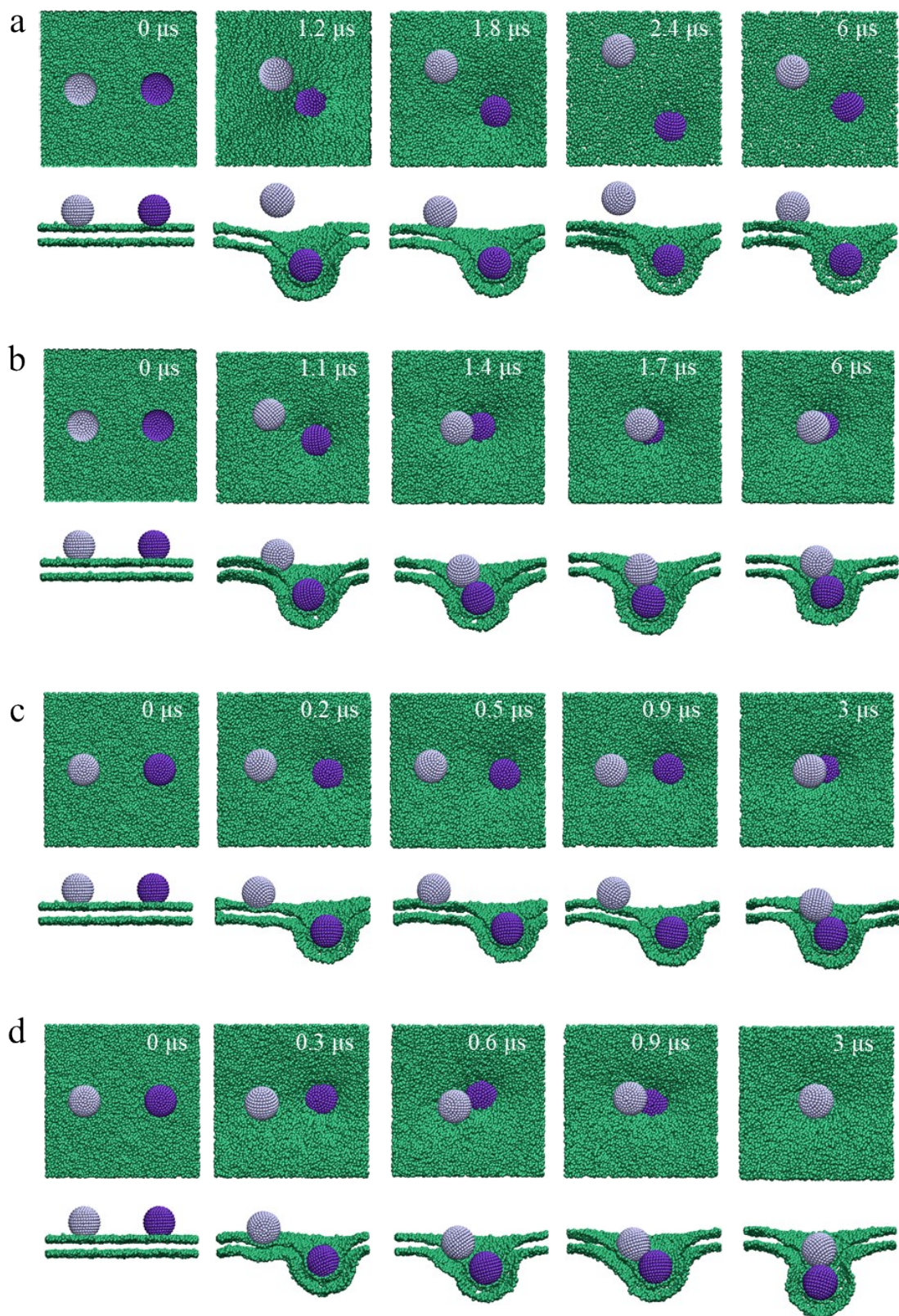


**Fig. S5** Representative snapshots showing the NP-membrane interactions with various  $\varepsilon_F$  and  $\varepsilon_B$ . (a)  $\varepsilon_F = 3.5 \text{ kJ/mol}$ ,  $\varepsilon_B = 1.0 \text{ kJ/mol}$ . (b)  $\varepsilon_F = 3.5 \text{ kJ/mol}$ ,  $\varepsilon_B = 1.5 \text{ kJ/mol}$ . (c)  $\varepsilon_F = 3.5 \text{ kJ/mol}$ ,  $\varepsilon_B = 2.0 \text{ kJ/mol}$ . (d)  $\varepsilon_F = 3.5 \text{ kJ/mol}$ ,  $\varepsilon_B = 2.7 \text{ kJ/mol}$ .  $\rho_F = \rho_B = 1.6 \text{ nm}^{-2}$ ,  $D_F = D_B = 8 \text{ nm}$ .

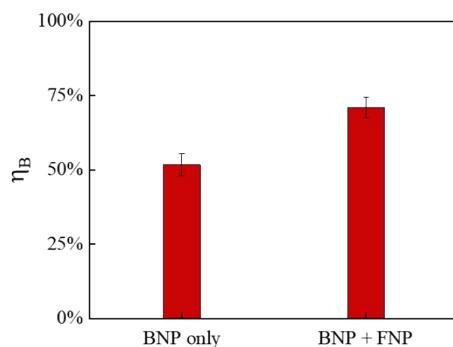


**Fig. S6** Membrane internalization degree of a BNP without or with a FNP.  $\varepsilon_F = 3.5 \text{ kJ/mol}$ ,  $\varepsilon_B = 2.7 \text{ kJ/mol}$ ,  $\rho_F = \rho_B = 1.6 \text{ nm}^{-2}$ ,  $D_F = D_B = 8 \text{ nm}$ .

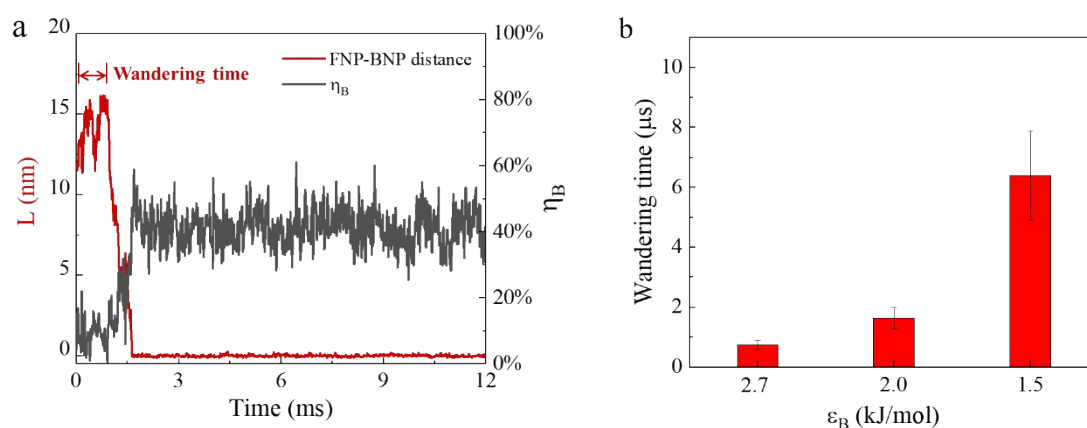


**Fig. S7** Motion of BNP in the bystander uptake process. (a) Changes of FNP-BNP distance and the membrane wrapping degree of the BNP. (b) Dependence of the wandering time of BNP on  $\varepsilon_B$ .  $\varepsilon_F = 3.5 \text{ kJ/mol}$ ,  $\rho_F = \rho_B = 1.6 \text{ nm}^{-2}$ ,  $D_F = D_B = 8 \text{ nm}$ . In (a),  $\varepsilon_B = 1.5 \text{ kJ/mol}$ .

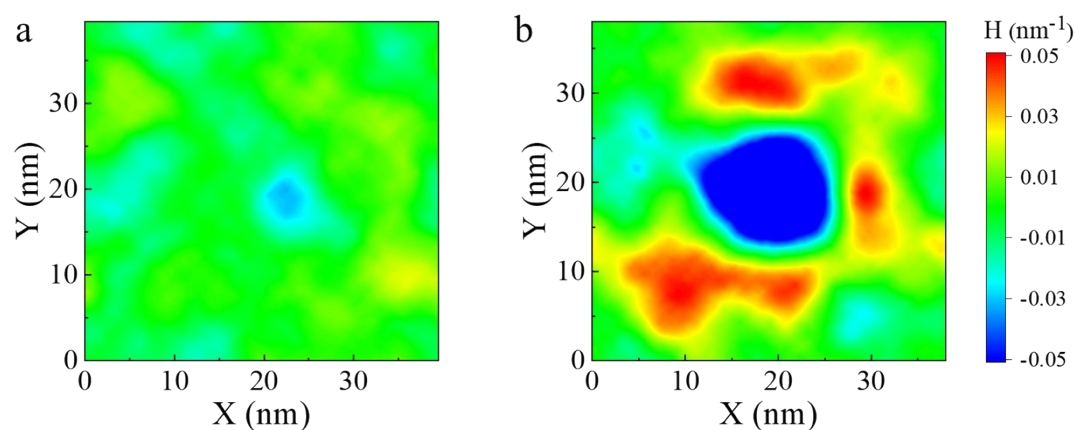


**Fig. S8** Curvature pattern of the membrane without (a) or with FNP (b).

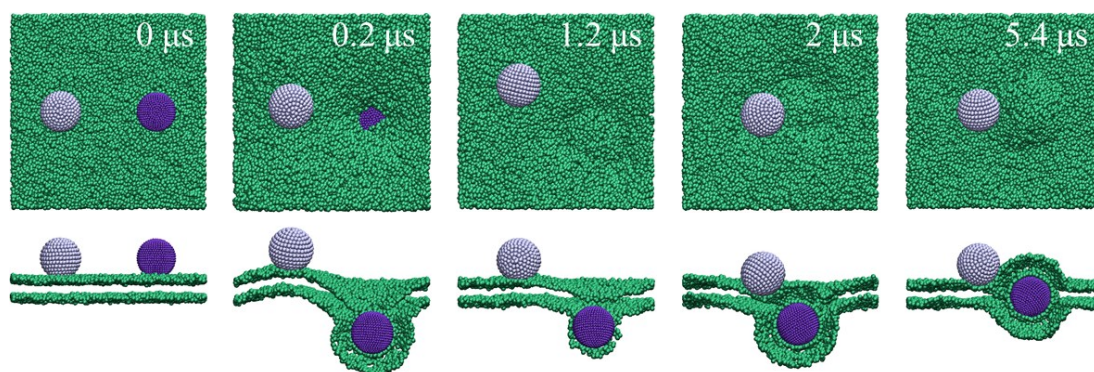


**Fig. S9** Influence of ligand density of FNPs on the bystander uptake effect. Representative simulation snapshots showing the NP-membrane interactions with a FNP having a quite large  $\rho_F$  value ( $\rho_F = 4.0 \text{ nm}^{-2}$ ),  $\varepsilon_F = 3.5 \text{ kJ/mol}$ ,  $\varepsilon_B = 1.5 \text{ kJ/mol}$ ,  $\rho_B = 1.6 \text{ nm}^{-2}$ ,  $D_F = D_B = 8 \text{ nm}$ .

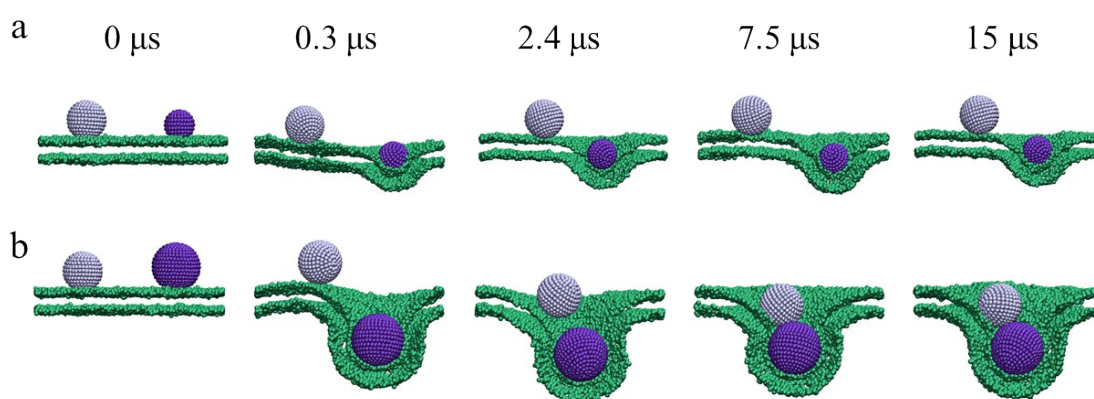


**Fig. S10** Effect of FNP size on the membrane internalization of BNPs. Representative simulation snapshots showing the NP-membrane interaction process with a FNP size of  $D_F = 6 \text{ nm}$  (a) or  $D_F = 10 \text{ nm}$  (b).  $\varepsilon_F = 3.5 \text{ kJ/mol}$ ,  $\varepsilon_B = 1.5 \text{ kJ/mol}$ ,  $\rho_F = \rho_B = 1.6 \text{ nm}^{-2}$ ,  $D_B = 8 \text{ nm}$ .



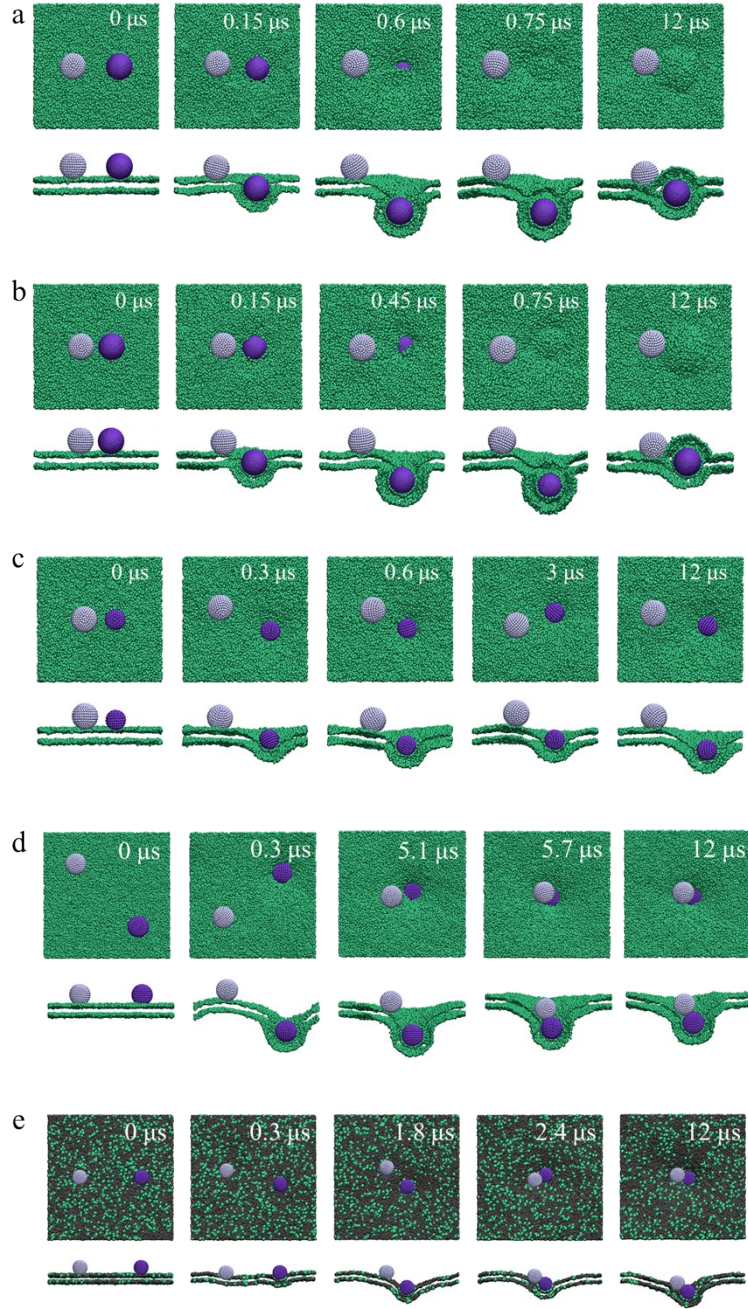


**Fig. S11** Representative simulation snapshots showing the minor influence of initial FNP-BNP distance on the bystander uptake effect. (a-b) Cases with a larger  $\rho_F$ . The initial FNP-BNP distance is 7 nm (a) or 2 nm (b).  $\varepsilon_F = 3.5 \text{ kJ/mol}$ ,  $\varepsilon_B = 1.5 \text{ kJ/mol}$ ,  $\rho_F = 4.0 \text{ nm}^{-2}$ ,  $\rho_B = 1.6 \text{ nm}^{-2}$ ,  $D_F = D_B = 8 \text{ nm}$ . (c) Case with a smaller  $D_F$ . The initial FNP-BNP distance is 2 nm.  $\varepsilon_F = 3.5 \text{ kJ/mol}$ ,  $\varepsilon_B = 1.5 \text{ kJ/mol}$ ,  $\rho_F = \rho_B = 1.6 \text{ nm}^{-2}$ ,  $D_F = 6 \text{ nm}$ ,  $D_B = 8 \text{ nm}$ . The initial FNP-BNP distance is 27 nm. Receptor density is 100% (d) or 10% (e).  $\varepsilon_F = 3.5 \text{ kJ/mol}$ ,  $\varepsilon_B = 1.5 \text{ kJ/mol}$ ,  $\rho_F = 4.0 \text{ nm}^{-2}$ ,  $\rho_B = 1.6 \text{ nm}^{-2}$ ,  $D_F = D_B = 8 \text{ nm}$ .

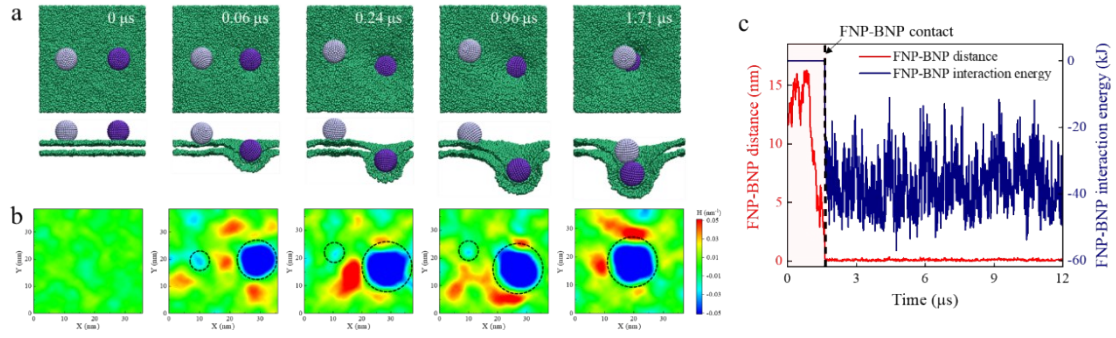


**Fig. S12** Analysis of membrane interaction process of FNP and BNP. (a) Snapshots showing the NPs-membrane interaction and the spontaneous movement of the BNP towards the FNP, and the corresponding membrane curvature patterns (b). (c) Corresponding FNP-BNP interaction and distance changes with time.  $\varepsilon_F = 3.5 \text{ kJ/mol}$ ,  $\varepsilon_B = 1.5 \text{ kJ/mol}$ ,  $\rho_F = \rho_B = 1.6 \text{ nm}^{-2}$ ,  $D_F = D_B = 8 \text{ nm}$ .

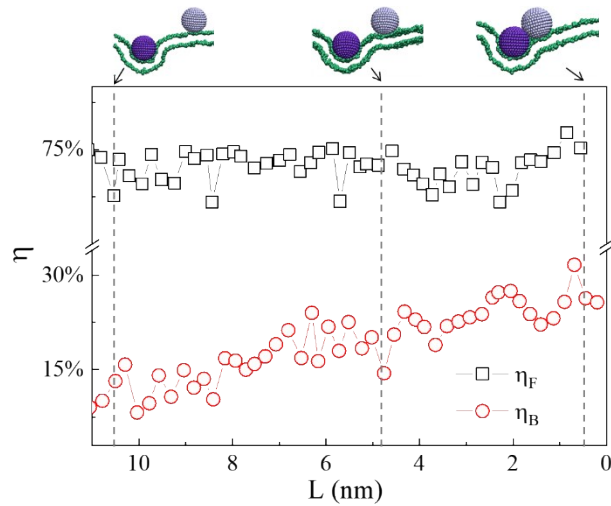


**Fig. S13** Membrane wrapping degrees of FNP ( $\eta_F$ ) and BNP ( $\eta_B$ ). For FNP,  $\eta_F$  is higher and stable; while for BNP,  $\eta_B$  increases with the decrease of FNP-BNP distance  $L$ .  $\varepsilon_F = 3.5 \text{ kJ/mol}$ ,  $\varepsilon_B = 1.5 \text{ kJ/mol}$ ,  $\rho_F = \rho_B = 1.6 \text{ nm}^{-2}$ ,  $D_F = D_B = 8 \text{ nm}$ .

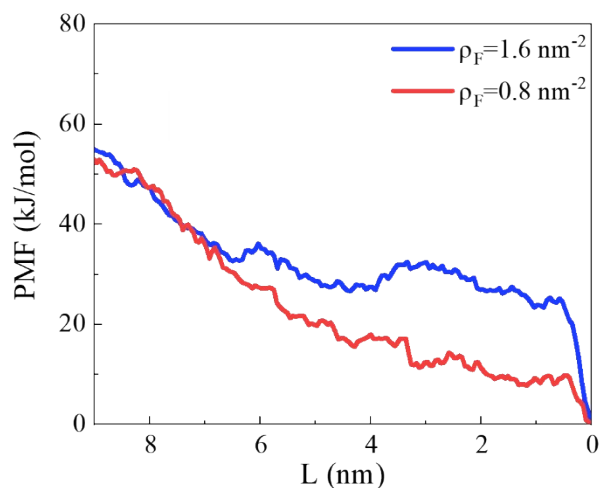


**Fig. S14** PMF profiles with varying  $\rho_F$  values.  $\varepsilon_F = 3.5 \text{ kJ/mol}$ ,  $\varepsilon_B = 1.5 \text{ kJ/mol}$ ,  $D_B = D_F = 8 \text{ nm}$ ,  $\rho_B = 1.6 \text{ nm}^{-2}$ ,  $\rho_F = 0.8 \text{ or } 1.6 \text{ nm}^{-2}$ .

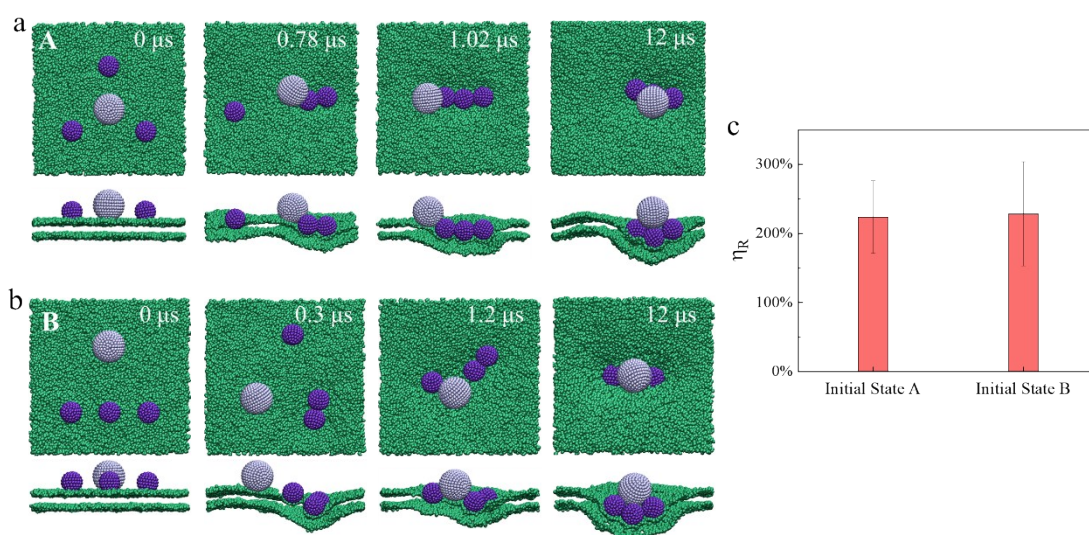


**Fig. S15** Effect of initial FNP configurations on the membrane internalization of BNPs. (a, b) Representative simulation snapshots showing the NP-membrane interactions. (c) Corresponding values of  $\eta_R$ .  $\varepsilon_F = 3.5 \text{ kJ/mol}$ ,  $\varepsilon_B = 1.5 \text{ kJ/mol}$ ,  $\rho_F = \rho_B = 1.6 \text{ nm}^{-2}$ ,  $D_B = 8 \text{ nm}$ ,  $D_F = 5 \text{ nm}$ .

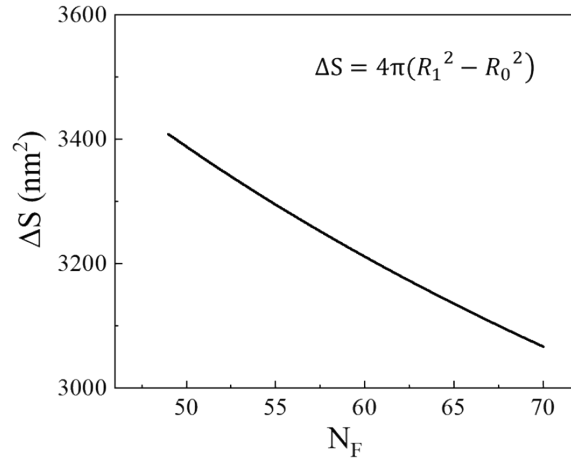


**Fig. S16**  $N_F$  dependent changes of the membrane area gain ( $\Delta S$ ).

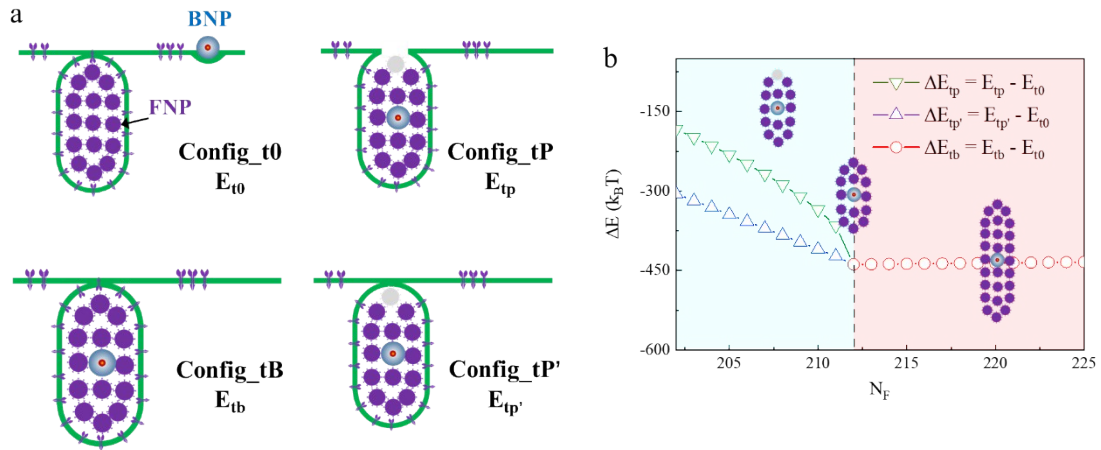


**Fig. S17** Energy analysis of the bystander uptake effect in a tube-like vesicle form. (a) Sketches showing some typical interaction states between the NPs (i.e., FNPs and BNPs) and the membrane. (b) Changes of energy differences between the different states with the FNP number  $N_F$ . Insets show the possible covering situations of FNPs around BNPs.  $N_B = 1$ ,  $r_F = 10 \text{ nm}$ ,  $r_B = 25 \text{ nm}$ .